Received: 11 January 2021 | Accepted: 17 March 2021 | Published: 22 April 2021
DOI:10.20870/oeno-one.2021.55.2.4588

Not just shrivelling: time-series profiling of the biochemical changes in Corvina (*Vitis vinifera* L.) berries subjected to post-harvest withering

Asfaw Degu[1,6*], Darren C. J. Wong[2], Gian Maria Ciman[3], Francesco Lonardi[3], Fulvio Mattivi[4,5] and Aaron Fait[6]

[1] Department of Plant Biology and Biodiversity Management, College of Natural and Computational Sciences, Addis Ababa University, Addis Ababa, Ethiopia.
[2] Ecology and Evolution, Research School of Biology, The Australian National University, Acton, ACT 2601, Australia.
[3] PerWine (Perfect Wine), Spin off University of Verona, Via della Pieve 70, 37029 San Floriano, Verona, Italy
[4] Department of Food Quality and Nutrition, Research and Innovation Centre, Fondazione Edmund Mach, San Michele all'Adige, Italy
[5] Department of Cellular Computational and Integrative Biology (CIBIO), University of Trento, Via Sommarive 9, 38123 Povo, Trento, Italy
[6] The French Associates Institute for Agriculture and Biotechnology of Drylands, the Jacob Blaustein Institute for Desert Research, Ben-Gurion University of the Negev, Sede Boqer 84990, Israel.

**corresponding author*: degua3@gmail.com

Associate editor: Luca Rolle

ABSTRACT

The grape berry withering process is often seen as a means to concentrate the constituents of the berry via water removal, however, recent molecular studies have indicated that the reprogramming of biosynthetic pathways that impart the unique aroma and flavour of the final wine also occur. Metabolic analysis was performed using GC-MS and LC-MS on Corvina berry dehydrated for up to 108 days. The temporal pattern of metabolic changes and time-series relationship between various classes of metabolites were investigated on berries sampled at 23-time points. Principal component analysis of both GC-MS and LC-MS datasets revealed three distinct phases of post-harvest withering; early (day 0–28), mid (day 35–66) and late (day 69–108) stages. Stress-associated amino acids such as proline, serine, ethanolamine, and leucine accumulated significantly during the mid and late stages of the drying process while phosphorylated glucose and fructose, sucrose, kestose and resveratrol increased massively across time. Unlike most of the identified metabolites, low molecular weight flavanols exhibited a consistent pattern of decline during the withering period. Our network analysis revealed that increased metabolic network connectivity occurred during the middle stage of withering, thus reflecting more coordinated metabolite changes while reduced network connectivity at early and late stages indicates minimal metabolite perturbation during these stages. The current prolonged berry withering experiment revealed the timing of metabolite interconversions in the central metabolism and provided critical clues that link the concentration effect, protein degradation, and the onset of stress-like conditions in drying berries.

KEYWORDS

Amarone, berry metabolism, berry withering, GC-MS, LC-MS

Supplementary data can be downloaded through: https://oeno-one.eu/article/view/4588

INTRODUCTION

The production of wines from partially dried grapes in the Veneto dates back to the times of the Ancient Romans. The structure of the berry renders low resistance to dehydration and enables berries of some selected grape varieties to shrivel under a slow withering process and leads to the development of the typical organoleptic characteristics of Amarone wine (Accordini, 2013). The appellation of origin controlled and guaranteed (DOCG) "Amarone della Valpolicella" is reserved for wines produced from autochthonous local cultivars including Corvina and/or Corvinone (from 45 % to 95 %), and Rondinella (from 5 % to 30 %), while up to 25 % can come from other red cultivars (MIPAAF, 2019). The rate of berry's water loss and the extent of metabolic changes including aroma compounds in Corvina, Corvinone and Rondinella grapes are quite different during the postharvest withering process (D'Onofrio *et al.,* 2019; Bellincontro *et al.,* 2016).

The postharvest withering of Corvina grape berry is a common practice for the production of the Amarone wine. The monovarietal wines from Corvina produced without withering have been described to be dominated by an unripe astringency and, at the same time, by a high relative contribution for surface smoothness in their astringency profile (Piombino *et al.,* 2020), and they have lower polyphenol levels and ethanol in comparison with most Italian red wines (Arapitsas *et al.,* 2020; Giacosa *et al.,* 2021). These characteristics of the cultivar are ideal for the production of a wine, Amarone, produced from partially dried grapes. The use of this traditional process dates back to the sixth century AD (Paronetto and Dellaglio, 2011). Berry withering process is usually done after harvest as an off-vine drying method (Mencarelli *et al.,* 2010; Panceri *et al.,* 2013). In the current Amarone wine production, a combination of natural and artificial ventilation practices transforms berries into partially dried fruit that can conserve and release desirable quality attributes during the vinification process (Bellincontro *et al.,* 2004). Indeed the biosynthesis of aroma and flavour of the final wine involves a series of complex biosynthetic pathways (Sanz *et al.,* 1996).

The post-harvest withering process of grapes lasts up to three months during which many withering-related metabolic changes undergo over time due to water loss (Kays, 1991). The final wine quality is mainly influenced by the accumulation of precursor metabolites during berry ripening and post-harvest withering. However, it has been shown that the speed of dehydration has a significant impact on the profile of volatile release in different grapevine varieties (Bellincontro *et al.,* 2004). Among the factors that may modulate the rate of water loss are the structural arrangement and composition of the grape berry skin wax layer (Possingham *et al.,* 1967; Dimopoulos *et al.,* 2020), but also environmental factors such as temperature, wind speed, and relative humidity (Kays, 1991; Roy *et al.,* 1999; Schirra *et al.,* 2000; Mencarelli *et al.,* 1994). All these elements could lead to metabolite compositional changes with a potentially detrimental impact on the final wine quality. Bellincontro *et al.* (2004) showed a reduction in volatile compounds while polyphenols show an increasing trend under a short-term withering experiment. Slaghenaufi *et al.* (2020) showed that the withering process is associated with the modulation of both fermentative and grape-related organic volatiles, including esters, higher alcohols, acids, C6 alcohols, terpenes and norisoprenoids. At the molecular level, water loss is associated with changes in cell wall enzyme activity (Hsiao, 1973), respiration and ethylene production (Kays, 1991). In the berry, these changes are known to take place (Costantini *et al.,* 2006; Zamboni *et al.,* 2008; Zenoni *et al.,* 2016) alongside transcriptome-wide reprogramming of metabolism pathways involving phytohormones, secondary metabolites, carbohydrate, and cell wall, as well as stress-protection, respiration, and transcriptional regulatory genes (Zenoni *et al.,* 2016). In the current study, MS-based profiling of primary and secondary metabolites was performed to characterize the withering-associated temporal pattern of metabolic changes in Corvina grapes.

MATERIALS AND METHODS

1. Berry sampling

Fully matured *V. vinifera* cv. Corvina grape berries were harvested on 25/09/2013 at Valpolicella (province of Verona, Italy), in a commercial vineyard of Monte dei Galli, San Pietro in Cariano, and withered for 108 days under controlled ventilation in the warehouse of Allegrini winery, located a few kilometres (< 5 km) away from the vineyard. A total of 23 samples were taken for metabolic analysis at different stages of the withering process and for each time-point of sampling, three biological replicates were collected.

For berry weight loss measurement, 7 trays (about 40 kg of grapes) were weighted at 20 sampling points (Supplementary Table S1).

2. Sample preparation and extraction for metabolite profiling

At each sampling stage during the withering process, 20 berries were randomly sampled, immediately snap-frozen with liquid nitrogen, and kept at −80 °C until further analysis. The grape berries (skin, flesh and seed together) were ground under liquid nitrogen using an IKA analytical mill (Staufen, Germany) to obtain a frozen powder and ahead of metabolite extraction, the frozen powder was freeze-dried in a lyophilizer. The freeze-dried samples were used for both primary and secondary metabolite analysis, according to a previously validated protocol (Theodoridis *et al.,* 2012).

3. Sample preparation and LC-MS targeted metabolomics.

An aliquot of 2 g of powder from each sample was extracted in sealed glass vials by adding 2400 µL of MeOH/H_2O (2:1), 1600 µL of chloroform and 40 µL of internal standard (gentisic acid and rosmarinic acid, 500 mg/L). The rosmarinic acid standard was used to adjust for the recovery, while gentisic acid was used to verify the stability within the sequence. The vials were put in an orbital shaker for 15 min at room temperature. Samples were centrifuged at 4000 g and 4 °C for 5 min, and the upper phase consisting of aqueous methanol was collected in a volumetric flask of 10 mL. Extraction was repeated by adding another 2400 µL of MeOH/H_2O) to the pellets and chloroform fractions. The upper phases from the second extraction were also added to the flask, the final volume of the combined extracts was brought to 10 mL, and filtered through a 0.2 µm PTFE filter before LC-MS analysis.

Quantitative, targeted analysis of phenolic metabolites was performed with a previously validated protocol by UPLC/QqQ-MS/MS (Vrhovsek *et al.,* 2012), with few modifications. A Waters™ Acquity UPLC system (Milford, MA) consisting of a binary pump, an online vacuum degasser, an autosampler and a column compartment was used. Phenolic compounds were separated at a temperature of 40 °C on a Waters™ Acquity HSS T3 column 1.8 µm, 150 mm × 2.1 mm (Milford, MA, USA). The mobile phase was composed of eluent A (0.1 % formic acid in water) and eluent B (0.1 % formic acid in acetonitrile), with a flow rate set to 0.4 mL/min. The multi-segment linear gradient elution conditions had the following steps: 0 min, 5 % B; from 0 to 3 min, to 20 % B; from 3 to 4.3 min, isocratic 20 % B; from 4.3 to 9 min, to 45 % B; from 9 to 11 min, to 100 % B; from 11 to 13 min, hold at 100 % B; from 13.01 to 15 min, the column was re-equilibrated to the initial conditions of 5 % B. The injection volume was 2 µL for both sample and standard solutions. Each sample was analyzed in triplicate. After each injection, the needle was rinsed with 600 µL of a weak washing solution (water/methanol, 90:10) and 200 µL of a strong washing solution (methanol/water, 90:10). Samples were kept at 6 °C during the analysis.

Mass spectrometry detection was performed on a Waters™ Xevo TQMS (Milford, MA, USA) instrument equipped with an electrospray (ESI) source. The capillary voltage was 3.5 kV in positive mode and −2.5 kV in negative mode; the source was kept at 150 °C ; the desolvation temperature was 500 °C ; cone gas flow, 50 L/h; and desolvation gas flow, 800 L/h. The MS parameters for MRM quantification are detailed in Vrhovsek *et al.* (2012). Quantification was done using Waters™ MassLynx 4.1 and TargetLynx software against a calibration curve made with pure standard.

4. GC-MS derivatization, run conditions and data processing

Tissue powder of 30 mg was transferred to a 2 mL tube, and metabolites were extracted in a pre-chilled methanol/chloroform/water extraction solution (2.5/1/1 v/v/v). From the upper water/methanol phase, 100 µL of the extract was dried in a vacuum concentrator (Eppendorf Concentrator Plus) for derivatization (Lisec *et al.,* 2006). The dried GC/MS samples were derivatized as described in Hochberg *et al.* (2013) with a similar retention time standard mix. The sample set also included a reference quality control of authentic metabolite standards (1 mg ml^{-1}, each) (Table S2). GC-MS run conditions were maintained exactly as described previously (Degu *et al.,* 2014). Volumes of 1 µL were then injected onto 30-m VF-5 ms GC column with 0.25 mm *i.d.*, film thickness of 0.25 µm, and +10 m EZ-Guard (Agilent) in splitless and split mode (32:1) allowing more accurate comparison of highly abundant metabolites (*e.g.*, sugars). The GC-MS system and the parameters of the machine were set exactly as described in (Degu *et al.,* 2014). Spectral searching was done by consulting the National Institute of Standards and Technology (NIST, Gaithersburg, USA) algorithm incorporated

in the Xcalibur® data software (version 2.0.7) against RI libraries from the Max-Planck Institute for Plant Physiology in Golm, Germany (Kopka *et al.,* 2004) and normalized by the internal standard ribitol.

5. Data analysis and statistical treatment

Principal component analysis (PCA) was applied to the entire data set after mean-centring and unit variance scaling using R (version 4.0.2) (R Core Team, 2020). Pairwise correlations to all identified metabolites for the three withering stages were performed separately using Pearson's correlation algorithm. The corresponding p-values were computed using the "cor.test" function of R as previously described (Toubiana *et al.,* 2012). Analysis of variance (ANOVA) was employed to analyse the effect of withering on metabolite accumulation among the three stages using R (version 4.0.2) (R Core Team, 2020).

Correlation-based network analysis was performed using a previously published method (Batushansky *et al.,* 2016). First, data from both platforms (GC- and LC-MS) was united, inspected on the missing values and divided into three groups based on PCA clustering: early (T1–T7), middle (T8–T14) and late (T15–T21). The first (T0) and the last (T22) time-points were excluded from the network analysis to equilibrate dimensions of the three groups, and avoid artificial differences between them during the comparative analysis. Next, Spearman's correlation matrices for each group separately were computed using "psych" package (Revelle, 2020) for R (Team, 2013) as described in Batushansky *et al.* (Batushansky *et al.,* 2016). Only correlation coefficients that passed the selected threshold ($r > |\pm 0.5|$, $p < 0.05$) were transformed to network format for visualization using Cytoscape (Shannon *et al.,* 2003). Graph theory-based network properties were calculated using the "igraph" package for R (Csardi and Nepusz, 2006).

RESULTS AND DISCUSSION

1. Metabolite profiling during post-harvest withering

GC-MS and LC-MS analysis identified a number of metabolites being altered in content during the post-withering process of Corvina berries. Metabolite profiling of both GC- and LC-MS based PCA plot clearly discriminated the long-term withering dataset into three distinct groups (Figure 1). Based on the PCA trajectories, the temporal pattern of metabolite changes during the withering process can be categorized into three phases; early (day 0–28), middle (day 35–66) and late (day 69–108) stage. Berry lost weight up to 16 %, 18–29 % and 30–36 % during the early, middle and late stages of withering, respectively (Table S3).

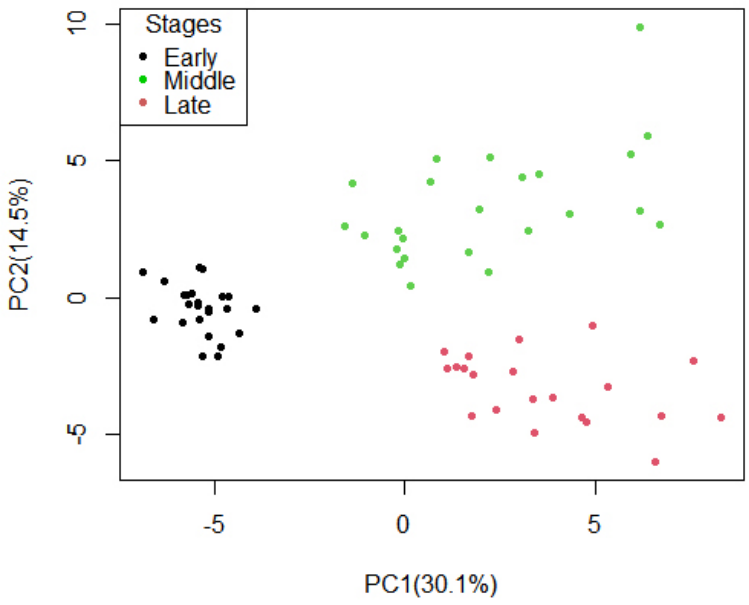

FIGURE 1. Change in central and specialized metabolite during berry withering of Corvina grape.
PCA plot of PC1 versus PC2 of GC/LC-MS metabolite profiles of Corvina grape berry during the three stages of berry withering. The percentage of the variance captured by each PC is given close to each respective axis. Each point in the plot represents one biological sample.

The first two principal components account for 44.6 % of the total variance (Table S3). The first principal component separated the early stage from the remaining two stages (middle and late), and the clustering was mainly due to sugars (Table S4). The latter two withering stages (middle and late) had similar trajectories along PC1 while they resolved on PC2, mainly due to differences in organic acids and hydroxycinamic acids (Table S4).

To clearly show the post-withering metabolite alteration, a fold-change of metabolites at the different drying stages relative to the initial time point (T_i) (harvest T_0) is displayed in Figures 2A, 2B and 3. Identified metabolites are grouped into sub-classes representing amino acids, organic acids, sugar acids, sugars, stilbenes, flavanols, flavonols, sugar alcohols and hydroxycinnamic acids. The levels to which the different metabolite classes accumulated during the withering process vary between these three mentioned phases. The largest magnitude of changes was observed within the mid and late stage of the dehydration process when the berry underwent 18–29 % and 30–36 % weight loss, respectively (Figures 2A,B and 3).

	Amino Acids							Am.a	Organic acid							In.ac	Sugar acid		Flavanol			Stilb.
# of days	Pyr(2TMS)	Val(2TMS)	Leu(2TMS)	Pro(2TMS)	Ala(3TMS)	Pro(+CO2) (2TMS)	Ser(2TMS)	Eth(3TMS)	MA(2TMS)	FA(2TMS)	MC(3TMS)	MI(3TMS)	ER(4TMS)	TA(4TMS)	CA(4TMS)	PA(3TMS)	GA(3TMS)	TH(4TMS)	Epi	Epi (5TMS)	Epig(6TMS)	tRes(3TMS)
0	1	1	1	1	1	1	1	1	1	1	1	1	1	1	1	1	1	1	1	1	1	1
6	1.0	1.0	1.0	1.7	0.7	1.2	1.8	2.1	1.0	0.9	1.1	0.9	0.8	1.0	1.2	1.0	1.3	0.6	0.3	0.4	0.5	2.2
10	1.0	1.0	1.0	1.6	0.6	1.5	0.7	1.0	1.1	0.9	1.3	1.1	0.8	1.1	1.2	1.3	1.3	1.1	0.9	0.7	0.3	1.9
14	1.6	1.2	1.2	2.0	1.9	2.7	3.8	0.9	1.0	0.9	1.3	1.0	0.7	1.1	1.2	1.0	1.3	0.7	0.6	0.6	0.4	5.3
17	0.7	0.8	0.8	1.3	0.6	1.6	0.8	0.8	1.2	0.8	1.1	1.2	0.7	1.0	1.3	1.4	1.5	1.2	0.6	0.5	0.3	3.9
21	0.9	0.9	1.0	2.5	0.9	2.1	1.5	1.0	1.3	0.8	1.3	1.1	0.6	1.1	1.3	1.3	1.3	0.9	0.4	0.4	0.4	3.2
24	0.6	0.7	0.8	1.0	0.8	1.2	0.4	3.7	1.0	0.9	1.2	0.9	0.6	0.9	1.2	1.2	1.4	0.8	0.8	0.6	0.2	2.6
28	0.8	0.8	0.7	1.6	1.0	1.8	0.4	1.0	1.5	1.0	1.4	1.5	0.7	1.1	1.7	1.2	1.5	1.3	0.6	0.4	0.4	5.9
35	1.5	1.3	2.4	6.7	0.3	0.4	5.1	13.1	1.7	1.6	1.5	1.3	1.2	1.6	2.0	2.3	2.5	1.2	0.8	1.0	1.8	35.6
41	1.6	3.0	3.1	10.6	0.4	0.7	7.8	12.6	1.7	1.8	1.6	1.3	1.3	1.4	2.1	2.3	2.2	1.4	1.3	0.7	0.4	10.8
45	1.1	1.1	2.1	4.9	0.3	0.6	4.0	13.8	1.6	1.4	1.7	0.9	1.1	1.5	1.8	2.4	2.1	1.0	0.8	0.8	0.8	67.3
52	1.8	1.6	2.5	19.3	0.6	1.3	8.1	11.7	1.6	1.4	1.9	1.3	1.7	1.4	1.9	2.2	1.8	1.5	1.6	1.3	0.5	42.0
56	1.4	3.0	4.6	17.8	0.6	1.1	8.0	14.6	1.9	2.0	1.9	1.6	2.2	1.7	2.6	3.4	2.8	1.9	1.1	1.0	0.6	948.1
59	1.8	3.8	4.5	31.9	0.8	1.1	8.2	14.4	2.1	2.3	1.7	1.7	3.0	1.9	2.9	4.0	2.8	2.4	1.1	1.1	0.9	92.5
63	1.3	3.1	3.7	20.2	0.5	1.1	5.4	15.2	1.9	2.1	1.5	1.6	2.9	2.1	2.8	4.4	2.9	2.1	2.5	2.0	1.1	1617
66	1.3	2.7	3.0	19.0	0.4	1.4	7.2	15.7	1.9	1.8	1.6	1.7	2.3	2.1	3.2	3.7	2.5	2.0	1.1	0.8	0.6	63.5
69	0.8	2.3	1.9	11.5	0.2	0.5	5.2	17.0	0.6	0.6	0.5	1.3	1.0	2.6	2.5	2.4	1.5	1.0	1.0	0.7	0.9	56.9
73	1.1	3.2	3.7	24.5	0.3	1.2	10.8	16.3	0.7	0.6	0.5	1.6	1.5	2.5	2.8	2.9	1.8	1.3	0.8	0.7	0.6	46.9
77	1.0	3.2	2.8	21.6	-	1.4	13.4	13.3	0.8	0.9	-	1.8	1.9	1.8	2.8	2.8	1.6	1.9	0.7	0.5	0.6	48.8
80	0.9	1.9	2.6	15.6	-	0.9	8.3	16.1	1.1	0.8	-	2.0	1.3	2.6	3.4	2.5	1.9	1.8	1.5	1.0	0.7	44.6
84	1.0	1.8	3.3	20.1	-	1.6	12.3	13.2	0.8	0.8	-	1.6	1.8	2.1	2.7	2.4	1.7	1.5	1.0	0.6	0.5	55.1
99	1.2	1.4	3.1	24.7	-	1.8	7.6	10.8	0.8	1.1	-	1.7	2.3	1.7	6.0	2.9	1.4	1.9	2.3	1.6	0.4	77.4
108	0.8	2.0	3.0	20.1	-	1.8	6.8	13.3	1.0	0.8	-	1.8	2.1	2.4	2.8	3.9	2.2	2.0	1.1	0.9	0.8	108.4

FIGURE 2A. Change in the relative abundance of GC-MS based metabolites according to the corresponding metabolic group during the post-harvest dehydration period.

The fold change values of metabolites relative to the initial time point are shown in the boxes and the colour of the box indicates the direction of changes as red (increased) or blue (declined). Each data point represents the means of three samples obtained from twenty berries. Values in each box represent fold change relative to day 0. "-" represents the metabolites that exist below the detection level. (Abbreviations: Pyr; Pyroglutamic acid, Val; Valine, Leu; Leucine, Pro; Proline, Ala; Alanine, Ser; Serine, Eth; Ethanolamine, MA; Maleic acid, FA; Fumaric acid, MC; Malonic acid, MI; Malic acid, ER; Erythronic acid, TA; Tartaric acid, CA; Citric acid, PA; Phosphoric acid, GA; Glyceric acid, FA; Fumaric acid, GA; Glyceric acid, TH; Threonic acid, Epi; Epicatechin, Epig; Epigallocatechin, tRes; trans Resveratrol)

2. Changes in amino acids and their derivatives during the withering process

Amino acids showed a mild change during the early stage of withering, with the exception of proline which showed an early increase up to 2.7-fold-change at 10 % weight loss (Figure 2A). During the mid (18–29 % weight loss) and late withering period (30–36 % weight loss), amino acids showed different patterns of changes. A significant difference in the accumulation of all identified amino acid occurred among the three withering stages (Table S5–S7). Pyroglutamate had mild change during early withering, accumulated moderately up to 1.8-fold change during mid-stage at 25 % weight loss, and showed mild change during the late withering phase. Parallel to the progressive water loss, proline level massively accumulated (up to 24-fold change at 31 % weight loss) a process that could be ascribed to stress-like conditions developing in the berry. Proline is one of the main water stress-related molecules in grapevine operating in the leaves (Hochberg *et al.,* 2013; Ju *et al.,* 2018), berries (Savoi *et al.,* 2017) and its progressive accumulation during the withering process is likely related to osmotic protection (Hong *et al.,* 2000; Bandurska, 2000), stabilizing membranes and preventing oxidative burst activities (Hayat *et al.,* 2012). Tholkappian *et al.* (2001) pointed out that water stress-associated conditions inhibit the utilization of amino acid in the downstream biosynthesis pathways and their build-up into protein. Due to such under-utilization, other amino acids such as serine, ethanolamine and leucine accumulated progressively during the mid and late stages of the drying process.

Plants synthesized ethanolamine directly from serine by serine decarboxylase enzyme in one reaction step and it plays an important role in the formation of cell membranes (Liu *et al.,* 2018). These phospholipid classes are essential membrane components in most biological organisms (Vance, 2015). The dehydration process accelerates the rate of respiration (Kays, 1991; Costantini *et al.,* 2006) and induces stress-like condition which facilitates the disintegration of biological membranes and could explain the accumulation of ethanolamine. Putrescine, the naturally occurring polyamine, is a well-known stress-associated amino alcohol, which notably increased (> 8 fold) during the mid and late stage of the withering. Similarly, environmental stress such as elevated temperature (Sweetman *et al.,* 2014) and water deficit (Savoi *et al.,* 2017) are also known to upregulate putrescine biosynthesis in grape berries. In other plants, Flores and Galston (1982) also pointed out a sharp increase in putrescine biosynthesis under osmotic stress. This result supports the previous prediction suggesting the role of polyamine in the re-generation of H_2O_2 for ROS-mediated drought stress responses (Alcázar *et al.,* 2011).

The other amino acids such as alanine, isoleucine, valine, beta-alanine, pyroglutamate, glutamate and arginine showed a moderate gradual increase. The general increase in amino-acid levels during the dehydration period could be due to the degradation of existing large protein molecules facilitated by proteases and peptidase released from damaged cells (Mandelstam, 1963; Yao *et al.,* 2006). Indeed, expression of enzymes encoding various aspartate-, subtilisin-, cysteine-, and serine proteases/peptidases, among others were not only highly expressed but also extensively modulated in several berry transcriptomes (*e.g.*, Corvina, Merlot, Sangiovese) subjected to postharvest dehydration (Zenoni *et al.,* 2016). This observation supports the hypothesis that as the protein degraded, amino acids will be available for the biosynthesis of new protein necessary for survival under stress conditions (Willetts, 1967). Alternatively, the cell might use the protein degradation process as a means to eliminate abnormal proteins formed as a result of stress. The increase in branched-chain amino acids (isoleucine, valine) presumably contributes to the peculiar aroma of Amarone wine as previously suggested in melon fruit (Gonda *et al.,* 2010).

3. Changes in organic acids and their derivatives during the withering process

Organic acids play an important role in the organoleptic properties of the final wine (Bauer and Dicks, 2004). Organic acids also influence wine stability, colour, and pH (Vilela, 2019). Similar to the amino acids, all the identified organic acids and their derivatives exhibited a significant difference in accumulation among the three stages (Table S5 – S7). During the early stage of withering (up to 16 % berry weight loss), levels of maleic acid, malonic acid, malic acid, erythronic acid, citric acid, tartaric acid, and fumaric acid showed only mild changes in the content; all exhibited moderate accumulation (up to 3.2 fold change at 29 % berry weight loss) during mid-stage of withering; during the late stage of withering maleic acid, malonic acid and fumaric acid showed progressive decline while

	Other Organic compound									Hydroxycin.		Sugars							Sugar alcohol		
# of days	PU(4TMS)	tCA, 4-OH(2TMS)	GLA(6TMS)	SA(6TMS)	TR(1TMS)	KE, 1-(11TMS)	GC	PCA(2TMS)	BAD(3TMS)	tSI(2TMS)	CF(3TMS)	Fru(1MEOX) (5TMS) MP	Fru(1MEOX) (5TMS) BP	Glu(1MEOX) (5TMS) MP	Glu(1MEOX) (5TMS) BP	F6P(6TMS) BP	G6P(6TMS) MP	Suc(8TMS)	Thr(4TMS)	Ery(4TMS)	mIN(6TMS)
0	1	1	1	1	1	1	1	1	1	1	1	1	1	1	1	1	1	1	1	1	1
6	1.4	1.2	0.8	1.5	1.3	1.6	1.1	0.8	1.0	0.7	0.9	1.1	1.0	1.0	1.0	1.2	1.3	0.8	1.1	1.0	0.8
10	1.3	1.3	0.9	1.5	0.9	1.5	1.2	0.9	0.9	0.6	1.3	1.1	1.0	1.0	1.0	1.3	1.3	1.1	1.2	1.2	0.8
14	1.2	1.4	0.8	1.2	0.9	1.5	1.0	0.8	0.8	0.5	1.1	1.0	0.9	0.9	0.9	1.3	1.2	1.0	1.1	0.9	0.8
17	0.8	1.3	1.3	0.7	1.0	1.7	1.2	0.9	1.0	0.4	1.1	1.2	1.1	1.1	1.2	1.5	1.5	1.1	1.2	1.0	0.7
21	1.3	1.5	0.7	2.3	1.3	2.0	1.3	1.0	1.1	0.3	1.3	1.2	1.2	1.2	1.2	1.3	1.3	1.2	1.3	1.1	0.7
24	1.3	1.2	0.5	1.8	1.0	1.6	1.2	1.0	1.1	0.3	0.9	1.3	1.3	1.4	1.4	1.4	1.3	0.7	1.2	1.0	0.8
28	1.0	1.3	0.9	1.2	1.0	2.7	1.3	0.9	1.0	0.3	1.1	1.2	1.2	1.2	1.2	1.5	1.5	1.2	1.2	1.1	0.6
35	1.9	2.8	1.2	3.0	5.7	6.6	4.6	2.5	1.9	1.5	2.3	1.2	1.1	0.9	0.9	2.4	2.7	1.8	1.7	1.5	0.9
41	2.0	2.4	1.2	2.7	5.8	6.5	4.2	2.3	1.8	1.1	2.0	1.2	1.0	0.9	0.9	2.4	2.8	1.6	1.9	1.7	0.7
45	2.6	2.7	1.0	3.6	4.8	7.5	4.6	2.0	1.9	0.8	2.4	1.2	1.0	0.8	0.9	2.9	3.1	1.6	2.2	1.7	0.7
52	4.7	2.1	1.5	2.6	3.7	10.2	2.8	2.0	1.7	0.6	1.8	1.1	0.9	0.8	0.8	2.8	3.4	1.6	2.2	1.7	0.9
56	4.3	4.6	1.3	5.3	5.4	13.8	4.9	2.4	1.8	0.7	2.3	1.2	1.1	0.9	0.9	4.2	5.1	1.8	2.4	1.7	1.0
59	8.3	2.8	1.5	4.7	9.4	13.2	7.7	2.9	2.1	0.8	2.3	1.5	1.3	1.2	1.1	3.8	4.9	2.4	2.7	1.9	1.0
63	5.4	2.8	2.1	3.9	8.2	16.5	8.1	3.2	2.5	0.6	2.4	1.7	1.4	1.2	1.2	5.0	6.1	2.5	2.8	1.9	1.0
66	4.9	2.9	1.8	3.8	6.8	15.7	5.3	2.5	2.2	0.6	2.0	1.6	1.4	1.2	1.2	4.6	6.6	2.4	2.7	1.8	1.0
69	4.0	1.7	1.0	4.2	3.4	11.7	6.4	0.5	0.7	1.1	1.7	3.1	3.0	2.6	2.1	5.9	7.1	4.5	2.4	2.0	0.7
73	3.1	1.6	1.0	5.3	4.7	12.4	4.3	0.5	0.7	0.4	1.5	2.6	2.6	2.2	1.8	4.8	6.4	3.7	2.1	1.7	0.7
77	5.5	1.3	1.4	5.4	4.5	12.8	4.3	0.6	0.7	-	1.3	2.1	2.2	1.9	1.5	6.8	7.6	3.2	2.2	1.8	1.0
80	2.5	1.8	1.5	4.4	4.5	11.5	4.0	0.5	1.0	-	1.3	2.7	2.8	2.2	1.9	7.3	8.4	3.9	2.2	1.6	1.0
84	2.7	1.4	1.3	3.1	3.1	13.2	4.0	0.5	0.7	-	1.1	2.2	2.2	1.9	1.5	5.2	6.0	3.1	2.2	1.7	0.8
99	5.2	1.2	1.4	4.4	3.2	16.4	3.2	0.5	0.7	-	0.9	1.9	1.8	1.7	1.3	8.1	8.4	2.6	2.4	2.2	0.9
108	4.4	1.7	1.9	5.7	3.7	22.0	4.5	0.5	0.8	-	1.3	2.4	2.4	2.1	1.6	8.3	8.9	3.7	2.2	2.0	1.0

FIGURE 2B. Change in the relative abundance of GC-MS based metabolites according to the corresponding metabolic group during the post-harvest dehydration period.

The fold change values of metabolites relative to the initial time point are shown in the boxes and the colour of the box indicates the direction of changes as red (increased) or blue (declined). Each data point represents the mean of three samples obtained from twenty berries. Values in each box represent fold change relative to day 0. "-" represents the metabolites that exist below the detection level. (Abbreviations: PU; Putrescine tCA, 4-OH; trans Cinnamic acid, 4-hydroxy GLA; Gluconic acid, SA; Saccharic acid, TR; Triazole, 4-methyl-5-hydroxyethy, KE; Kestose, GC; Glycolic acid, PCA; Pyrrole-2-carboxylic acid, BAD; Benzoic acid, 3,4-dihydroxy, tSI; synaptic acid trans, tCF; trans-Caffeic acid, Fru; Fructose, Glu; Glucos, F6P; Fructose-6-phosphate, G6P; Glucose-6-phosphate, Suc; Sucrose, Thr; Threitol, Ery; Erythritol, mIN; myo-Inositol)

malic acid, erythronic acid, citric acid, tartaric acid maintained moderate levels (Figure 2B).

Similarly, cinnamic acid derivatives such as cinnamate, caffeate and synapate also showed a transit peak during the dehydration process. Hydroxylated benzoate also showed a transit peak followed by a significant reduction towards the end of the dehydration period. Organic acid biosynthesis is central to carbon metabolism producing precursors in the biosynthetic route of diverse compounds such as amino acids, vitamins, polyphenols and terpenic aroma volatiles. Therefore, the observed mild changes during withering probably reflect a reduction in the utilization of metabolites in the aforementioned downstream biosynthetic pathways any further.

4. Changes in sugars and their derivatives during the withering process

As expected, progressive water loss caused a significant concomitant sugar accumulation, particularly sugar phosphates, fructose 1,6-bisphosphate (F1,6—BP) and glucose 1,6-bisphosphate (G1,6-BP) which increased up to 9-fold changes towards the end of withering (36 % berry weight loss) while sucrose increased moderately during the mid-stage (29 % berry weight loss) and up to 4.5-fold-change during the late stage of withering (30 % berry weight loss) (Figure 2B). The general increase in sugar levels during withering is likely associated with the dehydration process though the accumulation of sugar in the berry is regulated by complex mechanisms and poorly understood (Delrot *et al.,* 2000). The general increase in sugar contents in our study (Figure 2B) is in accordance with Reščič *et al.* (2016), suggesting the changes in soluble sugar accumulation is the foremost change during the post-harvest withering process. Unlike pre-harvest accumulation of soluble carbohydrates in berries, which are imported into the fruit as photoassimilate, the progressive increase in sugars during the post-harvest withering period mostly associated with the loss of water during withering and anaerobic metabolism as previously suggested by Costantini *et al.* (2006). Thus, the withering process favoured a sugar concentration, which may lead to fine alcoholic Amarone wine with a characteristic flavour.

5. Changes in stilbene and other health-promoting compounds during the withering process

Another general effect of the post-harvest withering process is the significant accumulation of stilbene compounds including cis-piceide, trans-piceide and trans-resveratrol (Figures 2A and 3). Corvina grapes are rich in resveratrol, and a strong increase in these compounds in both the grapes and the wines can be elicited by the UV-C radiation during the withering (Paronetto and Mattivi, 1999). The modulation of this pathway has emerged as one of the key effects also in our trial. Particularly, trans-resveratrol had a massive induction (> 100-fold change at 36 % berry weight loss) from the initial time point (Figure 2A), suggesting improved nutritional status of raisin grape during the period of withering. Similarly, several reports (*e.g.*, Versari *et al.* 2001; Mencarelli *et al.* 2010; Zenoni *et al.* 2016) also reported that post-harvest berry withering induced the accumulation of stilbene compounds. It is well established that multiple factors including grape cultivar, genotype, location, environmental conditions attribute for the variation of grape berry stilbene compound accumulation. Nevertheless, extensive transcriptome analysis of post-harvest withering grapes (Zamboni *et al.,* 2008; Zenoni *et al.,* 2016) indicated induction of a large suite (> 40) of stilbene synthase genes (Vannozzi *et al.,* 2012) as well as their transcriptional regulators such as MYB14/15 (Höll *et al.,* 2013) and WRKY03/24 (Vannozzi *et al.,* 2018). In addition, the withering process massively induced the fermentation of alcoholic product, triazole, 4-methyl-5-hydroxyethyl, over time. This result likely indicates a progressive decline in oxygen level in the drying berry and leads to the accumulation of anaerobic fermentation products. Triazole and its derivatives possess health-promoting properties including antimicrobial, antihypertensive, antiviral, antioxidant, antitumor and anti-inflammatory (Rauf and Farshori, 2011).

6. Changes in flavonoids during the withering process

Unlike the other metabolite classes, most of the flavanol and flavonol metabolite classes did not show a significant difference among the three withering stages (Table S5–S7). A consistent decrease in the levels of metabolites in flavanols class including catechin, gallocatechin, epicatechin, epigallocatechin (5TMS) and epigallocatechin (6TMS) procyanidin B1 and B2 is one of the prominent change of the post-harvest withering (Figures 2A and 3). This finding is in agreement with a previous report showing a progressive decline in flavanols during Corvina berry withering (Versari *et al.,* 2001). An increase in polyphenol oxidase during the postharvest withering process (Bonghi *et al.,* 2012; Rolle *et al.,* 2009) might be associated with the decline in flavanol compounds. Metabolites in the flavonol group including kaempferol glucoside, quercetin glucoside, dihydrokaempferol, quercetin galactoside, kaempferol glucoside, syringetin galactoside, isorhamnetin galactoside and rutin exhibited a general increase during the withering process whereas myricetin exhibited a consistent declining trend. Previous sensory analysis suggested that flavonols were among the compounds responsible for the velvety astringency of Amarone wines, having recognition threshold concentrations in the range 0.2 to 4.8 μmol/L (Hufnagel and Hofmann, 2008a), and the velvety character is a distinctive sub-quality of the taste of Corvina wines (Piombino *et al.,* 2020).

In the field time-series experiment, Shojaie *et al.* (2016) reported that the amount of flavonol was significantly higher under severe drought stress than its amount under control conditions or mild drought stress, suggesting that flavonols are potential mitigators for drought stress (Shojaie *et al.,* 2016). Reščič *et al.* (2016) reported that the increase in phenolics due to dehydration of grape berries resulted in higher levels of these compounds in the final wines compared to the control. The post-harvest withering process may advance the phenolic ripening, leading to higher levels of phenolic compounds in withered berries. Nevertheless, compared to the pre-harvest massive flavonoid accumulation where the upstream genes regulate the pathway in a coordinated pattern (Chen *et al.,* 2017), the general moderate increase in our study could be ascribed to the concentration effect caused by the withering of berries.

	Flavonols									Cinamic Acid				Flavanols						Stilbenes	
# of days	Kamp glc.	Quer gluc	Dihydrokaem	Quer glc	Kaemp gluc	Syringetin glc	Isorhamnetin glc	Myricetin	Rutin	Caftarate	Fertarate	Gallate	Coutarate	Catechina	Epicatechina	Gallocatechin	Epigallocatechin	Procyanidin B1	Procyanidin B2	trans-Piceide	cis-Piceide
0	1.0	1.0	1.0	1.0	1.0	1.0	1.0	1.0	1.0	1.0	1.0	1.0	1.0	1.0	1.0	1.0	1.0	1.0	1.0	1.0	1.0
6	1.3	1.2	1.6	1.2	1.3	0.8	1.1	0.7	1.5	0.9	0.9	0.8	0.8	0.7	0.8	0.8	0.7	0.7	0.9	1.2	1.0
10	1.1	1.2	1.3	1.1	0.9	0.8	1.1	0.9	1.3	1.1	0.9	0.9	0.9	0.8	1.0	0.5	0.8	0.7	1.0	1.0	0.7
14	1.2	1.1	1.4	1.2	1.3	1.0	1.2	1.0	0.9	1.1	0.9	1.0	0.8	0.5	0.5	0.5	0.7	0.6	0.9	1.1	1.3
17	0.8	1.0	1.1	0.9	0.9	0.7	0.9	0.7	0.9	1.0	0.9	0.7	0.8	0.5	0.6	0.4	0.7	0.6	0.8	2.7	2.0
21	1.1	1.0	1.6	1.1	1.0	0.8	1.1	0.9	1.1	1.2	1.0	0.4	1.0	0.4	0.3	0.6	0.7	0.8	0.8	0.7	0.3
24	1.2	1.6	1.4	1.1	1.6	1.3	1.3	0.6	1.9	0.4	0.9	1.6	0.2	0.3	0.6	0.3	0.5	0.6	0.8	0.5	0.1
28	0.3	0.6	1.2	0.5	0.3	1.3	0.5	0.6	0.4	1.1	1.1	0.9	1.1	0.5	0.9	0.7	0.8	0.9	1.2	0.7	0.4
35	0.7	1.0	1.4	0.9	0.8	1.5	1.0	0.7	1.0	1.1	1.0	0.8	0.9	0.3	0.9	0.3	0.7	0.8	1.2	4.6	3.4
41	1.2	1.1	1.4	1.3	1.2	0.9	1.3	0.7	1.3	1.1	0.9	0.7	0.7	0.3	0.4	0.2	0.7	0.6	0.9	2.2	1.1
45	1.7	1.8	1.5	1.7	1.9	1.8	2.0	0.4	1.8	1.2	1.0	0.8	0.6	0.4	0.5	0.3	0.5	0.8	1.0	8.6	5.6
52	1.2	1.2	1.6	1.3	1.1	1.4	1.1	0.5	1.5	1.1	1.1	0.8	1.0	0.4	0.8	0.2	0.7	0.8	1.2	1.1	0.5
56	1.0	0.9	1.4	1.1	0.9	1.3	1.1	0.4	0.8	1.1	1.0	1.0	0.9	0.6	1.9	0.2	0.7	0.7	1.3	5.1	3.0
59	1.6	1.3	1.6	1.7	1.5	1.1	1.7	0.6	1.3	1.1	1.1	1.0	0.9	1.0	0.9	0.2	0.6	0.8	1.4	2.5	1.1
63	1.3	1.4	1.8	1.3	1.4	1.2	1.3	0.4	1.6	1.2	1.1	0.7	0.7	0.6	0.7	0.2	0.7	0.6	0.9	2.8	1.7
66	1.0	1.0	1.3	1.2	0.9	0.9	1.1	0.4	1.0	1.1	1.0	0.7	0.8	0.4	0.8	0.2	0.6	0.5	0.9	1.9	1.2
69	0.6	1.0	1.3	0.8	0.8	1.4	0.9	0.5	1.1	1.1	1.1	0.9	0.7	0.5	1.2	0.3	0.6	0.7	1.2	8.2	6.8
73	1.0	1.0	1.6	1.3	0.8	1.4	1.6	0.5	0.9	1.2	1.2	2.5	0.8	0.4	0.5	0.2	0.7	0.7	1.2	2.7	1.8
77	1.6	1.8	1.5	1.6	1.5	1.4	1.6	0.3	2.3	1.3	1.2	0.6	0.7	0.4	0.5	0.2	0.6	0.7	1.0	6.6	4.0
80	1.3	1.7	1.6	1.3	1.5	1.6	1.2	0.5	2.2	1.3	1.2	1.8	0.7	0.3	0.4	0.3	0.6	0.7	0.9	4.9	2.2
84	0.9	1.3	1.6	1.2	1.2	1.5	1.2	0.6	1.2	1.2	1.2	0.5	0.8	0.4	0.6	0.2	0.5	0.6	1.3	5.1	2.4
99	2.1	1.8	2.2	2.3	2.1	1.7	2.2	0.6	2.8	1.1	1.3	0.7	0.8	0.7	0.7	0.2	0.6	0.8	1.4	3.7	1.0
108	1.4	1.6	1.7	1.5	1.5	1.5	1.5	0.3	2.1	1.2	1.2	1.1	0.9	0.6	0.6	0.2	0.5	0.6	1.2	6.0	4.8

FIGURE 3. Change in the relative abundance of LC-MS based metabolites according to the corresponding metabolic group during the post-harvest dehydration period.

Each data point represents the means of three samples obtained from twenty berries. Values in each box represent fold change relative to day 0 or when the first detection level of the metabolite is recorded. «-» represents the metabolites that exist below the detection level.

7. Metabolite network and correlation analysis

To investigate systematic changes occurring during berry withering a correlation-based network analysis was performed on three sets of data profiles from the three phases of withering. It is well known that dramatic physiological, metabolic and textural changes characterize berry ripening following veraison. The classical analysis of metabolite profile demonstrated distinct patterns of changes in different compound classes during the long-term berry withering. Correlation-based network analysis revealed that extensive topological differences exist among the three networks of withering stages.

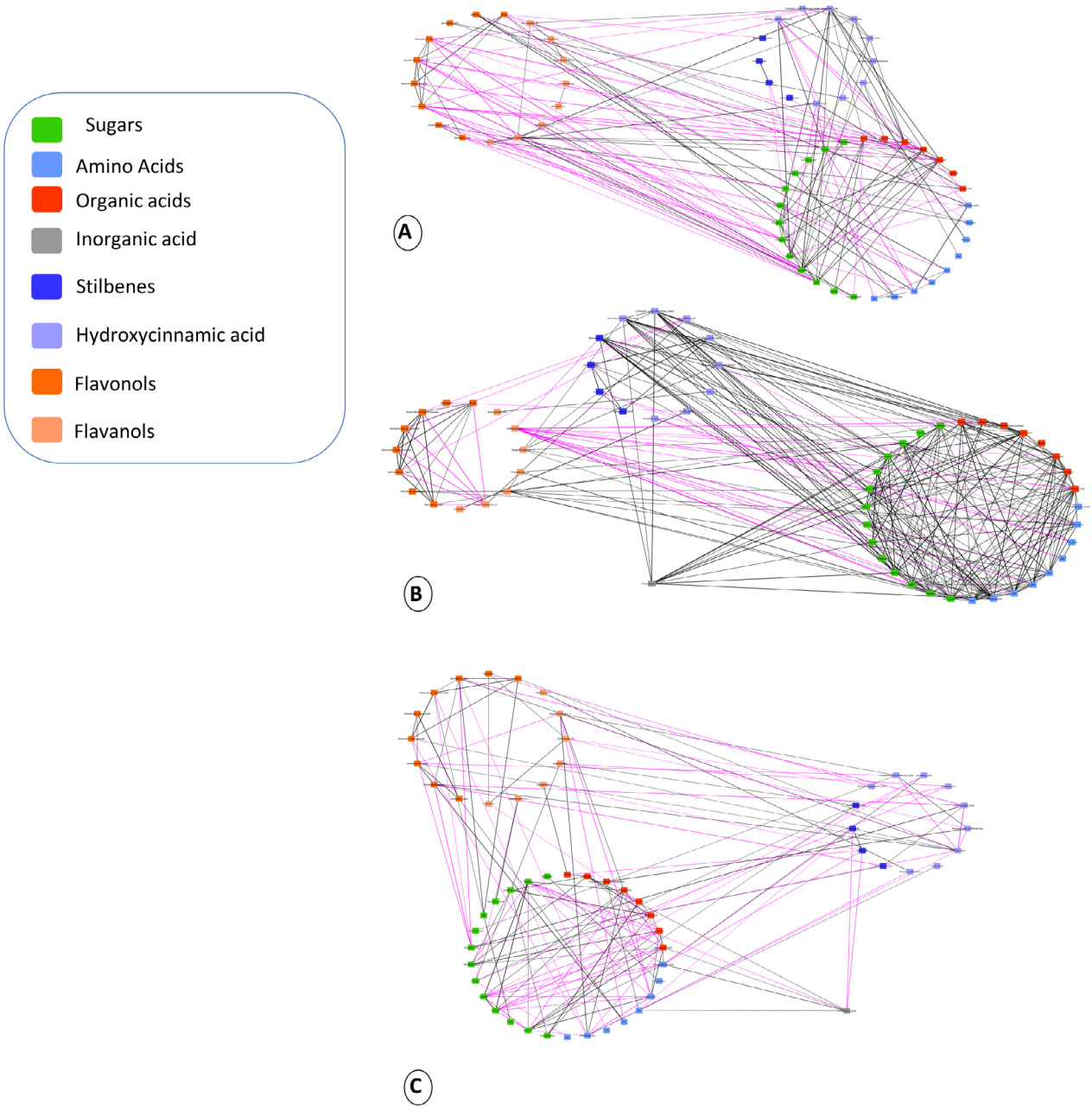

FIGURE 4. Metabolite correlation-based network analysis during the early (A), mid (B) and late (C) stages of berry withering.

Nodes correspond to the different metabolite classes; node colours correspond to compound classes as detailed in the figure legend. Edges between nodes are correlation coefficients that passed the selected threshold ($r > |\pm 0.5|$, $p < 0.05$), where pink and dark edges correspond to negative and positive correlations, respectively.

TABLE 1. Main graph theory-based properties of the metabolic correlation-based networks.

Network	Vertices	Edges (pos:neg in %)	Density	Diameter
Early	59	159 (62:38)	0.09	9
Mid	59	267 (88:12)	0.16	6
Late	60	143 (56:44)	0.08	9

As the withering process advances from early (up to 16 % berry weight loss) to middle phase (18–29 % berry weight loss), it increased the number of edges from 159 to 267, and network density from 0.09 to 0.16 (Table 1). This reflects that the berry underwent minimal metabolic rearrangements during the early stage may be due to mild water loss (Supplementary Table S1). Further water loss towards the late withering stage (30–36 % berry weight loss) markedly dropped the number of edges from 267 to 143 and network density, from 0.16 to 0.08. During the middle stage of withering, however, the berry underwent a massive coordinated metabolic rearrangement perhaps due to larger water loss leads to protein degradation and activation of stress-related biosynthetic pathways. During the late stage of withering, the decrease in network connectivity and network density might be associated with a reduction in the aforementioned biological processes. Diameter (the longest/shortest pathways between any two nodes in the graph) of the metabolic networks at early and late phases were remarkably higher compared to the middle (9 *vs*. 6, respectively) supporting weak interaction during early and late stages of withering. Interestingly, early and late stages networks demonstrated remarkable similarity in main properties; including the proportion of positive and negative integrations between metabolites (~60:40), while the middle stage network was characterized by the overwhelmingly high number of positive interactions (88 %). The current networks analysis also revealed that strong connectivity between compounds were obtained in the networks of primary biosynthetic pathways. Surprisingly, specialized metabolites like flavonoids and phenylpropanoids are more connected with primary metabolites than with each other. Several studies have shown that environmental stress significantly influences the network connectivity of metabolites in various grapevine tissues. For example, water deficit stress was previously shown to increase the network connectivity of primary and secondary metabolites in grape berries (Savoi *et al.,* 2017) and leaves (Hochberg *et al.,* 2013). Nonetheless, the phenomenon observed here distinguishes the postharvest dehydration metabolism from the general pre-harvest berry ripening process (Degu *et al.,* 2014) and deficit irrigation in leaves (Hochberg *et al.,* 2013) that mainly links primary metabolism from the downstream specialized metabolites (Hochberg *et al.,* 2013).

To gain insight into the relationship between different metabolite classes during the berry withering process both the LC- and GC-MS dataset were used in the correlation analysis (Table S8A – 9C). Furthermore, correlation coefficient heat map of metabolites for the three withering stages were generated using the R corrplot package (Figure S1 – S3). There were highly significant positive (Table S8A – S9C) correlations between ethanolamine with sugars like fructose (r = 0.9), glucose MP (r = 0.85), glucose BP (r = 0.92) and sucrose (r = 0.89) during the late stage of withering. Similar correlation values were observed during the mid-stage of withering. The correlation of tartrate with sugars also exhibited similar correlation trends during the mid and late stages of withering. These metabolites belong to different metabolic classes but showed a progressive increase during the withering process (Figure 2A, 2B) suggesting a dehydration-driven concentration of metabolites in the berries.

CONCLUSIONS

In conclusion, Corvina grape berry undergoes a pronounced shift in metabolism in response to the prolonged withering period with the accumulation of stress-related amino acids, sugars, organic acids, flavonols, stilbene compounds and ethanolamine while the flavanols declined over time. These changes define the body and flavour of the final wine. The general increase in sugars and organic acids during the withering process perhaps is likely due to the concentration effect through the decrease in berry weight. Alternatively, stress markers like resveratrol and proline exhibited a massive increase more than the concentration effect and perhaps associated with the stimulation of different genes involved in stress protection mechanisms due to water loss. The metabolite data presented here reveal the timing of important switches in both central and specialized metabolites in the withering process, which can potentially be related to wine flavour composition and production of wines with distinct styles.

Acknowledgement: We are grateful to Prof. Roberto Ferrarini, deceased in November 2014, who conceived and had a central role in every stage of this project. We would like also to thank Dr Albert Batushansky for his kind help in the network analysis and Daniele Perenzoni for his support in LC-MS/MS analysis of polyphenols. FM acknowledges the support of the Autonomous Province of Trento, project AdP 2015. AF and AD acknowledge the support of the Blaustein Center for Scientific Cooperation (BCSC).

Funding Sources: This research was granted by the Autonomous Province of Trento, project AdP 2015.

Supporting Information: Weight loss measurements during the withering process (Table S1), list of authentic standards used for GC-MS analysis (Table S2), PCA analysis PC proportion and eigenvalues (Table S3 and S4), LC-MS and GC-MS based metabolite raw data (Table S5), metabolite mean + standard deviation (Table S6), ANOVA analysis of metabolites (Table S7), metabolites correlation and P values for the three stages (Table S8A–S9C), correlation heat map between metabolites (Figure S1 – S3).

REFERENCES

Accordini, D. (2013). Amarone. In: Mencarelli, F., & Tonutti, P. (2013). *Sweet, reinforced and fortified wines*. Wiley-Blackwell, John Wiley and Sons, UK. https://doi. org/10.1002/9781118569184.

Alcázar, R., Bitrián, M., Bartels, D., Koncz, C., Altabella, T., & Tiburcio, A. F. (2011). Polyamine metabolic canalization in response to drought stress in Arabidopsis and the resurrection plant Craterostigma plantagineum. *Plant Signaling & Behavior*, *6*(2), 243–250. https://doi. org/10.4161/psb.6.2.14317

Arapitsas, P., Ugliano, M., Marangon, M., Piombino, P., Rolle, L., Gerbi, V., Versari, A., & Mattivi, F. (2020). Use of Untargeted Liquid Chromatography--Mass Spectrometry Metabolome To Discriminate Italian Monovarietal Red Wines, Produced in Their Different Terroirs. *Journal of Agricultural and Food Chemistry*. https://doi. org/10.1021/acs.jafc.0c00879

Bandurska, H. (2000). Does proline accumulated in leaves of water deficit stressed barley plants confine cell membrane injury? I. Free proline accumulation and membrane injury index in drought and osmotically stressed plants. *Acta Physiologiae Plantarum*, *22*(4), 409–415. https://doi. org/10.1007/s11738-000-0081-7

Batushansky, A., Toubiana, D., & Fait, A. (2016). Correlation-based network generation, visualization, and analysis as a powerful tool in biological studies: a case study in cancer cell metabolism. *BioMed Research International*, *2016*. https://doi. org/10.1155/2016/8313272

Bauer, R., & Dicks, L. M. T. (2004). Control of malolactic fermentation in wine. A review. *South African Journal of Enology and Viticulture*, *25*(2), 74–88. https://doi. org/10.21548/25-2-2141

Bellincontro, A., Matarese, F., D'Onofrio, C., Accordini, D., Tosi, E., & Mencarelli, F. (2016). Management of postharvest grape withering to optimise the aroma of the final wine: A case study on Amarone. Food chemistry, 213, pp.378-387. https://doi. org/10.1016/j.foodchem.2016.06.098

Bellincontro, A., De Santis, D., Botondi, R., Villa, I., & Mencarelli, F. (2004). Different postharvest dehydration rates affect quality characteristics and volatile compounds of Malvasia, Trebbiano and Sangiovese grapes for wine production. *Journal of the Science of Food and Agriculture*, *84*(13), 1791–1800. https://doi. org/10.1002/jsfa.1889

Bonghi, C., Rizzini, F. M., Gambuti, A., Moio, L., Chkaiban, L., & Tonutti, P. (2012). Phenol compound metabolism and gene expression in the skin of wine grape (*Vitis vinifera* L.) berries subjected to partial postharvest dehydration. *Postharvest Biology and Technology*, *67*, 102–109. https://doi. org/10.1016/j.postharvbio.2012.01.002

Chen, W.-K., Bai, X.-J., Cao, M.-M., Cheng, G., Cao, X.-J., Guo, R.-R., Wang, Y., He, L., Yang, X.-H., He, F., Duan, C.-Q., & Wang, J. (2017). Dissecting the variations of ripening progression and flavonoid metabolism in grape berries grown under double cropping system. *Frontiers in Plant Science*, *8*, 1912. https://doi. org/10.3389/fpls.2017.01912

Costantini, V., Bellincontro, A., De Santis, D., Botondi, R., & Mencarelli, F. (2006). Metabolic changes of Malvasia grapes for wine production during postharvest drying. *Journal of Agricultural and Food Chemistry*, *54*(9), 3334–3340. https://doi. org/10.1021/jf053117l

Csardi, G., & Nepusz, T. (2006). The igraph software package for complex network research. *InterJournal, Complex Systems*, *1695*(5), 1–9.

Degu, A., Hochberg, U., Sikron, N., Venturini, L., Buson, G., Ghan, R., Plaschkes, I., Batushansky, A., Chalifa-Caspi, V., Mattivi, F., & Fait, A. (2014). Metabolite and transcript profiling of berry skin during fruit development elucidates differential regulation between Cabernet-Sauvignon and Shiraz cultivars at branching points in the polyphenol pathway. *BMC Plant Biology, 14, 188*. https://doi. org/10.1186/s12870-014-0188-4

Delrot, S., Atanassova, R., & Maurousset, L. (2000). Regulation of sugar, amino acid and peptide plant membrane transporters. *Biochimica et Biophysica Acta (BBA)-Biomembranes*, *1465*(1–2), 281–306. https://doi. org/10.1016/S0005-2736(00)00145-0

Dimopoulos, N., Tindjau, R., Wong, D. C. J., Matzat, T., Haslam, T., Song, C., Gambetta, G. A., Kunst, L., & Castellarin, S. D. (2020). Drought stress modulates cuticular wax composition of the grape berry. *Journal of Experimental Botany*, *71*(10), 3126–3141. https://doi. org/10.1093/jxb/eraa046

D'Onofrio, C., Bellincontro, A., Accordini, D. & Mencarelli, F. (2019). Malic acid as a potential marker for the aroma compounds of amarone winegrape varieties in withering. American Journal of Enology and Viticulture, 70(3), pp.259-266.

Flores, H. E., & Galston, A. W. (1982). Polyamines and plant stress: activation of putrescine biosynthesis by osmotic shock. *Science*, *217*(4566), 1259–1261. https://doi. org/10.1126/science.217.4566.1259

Giacosa, S., Parpinello, G.P., Segade, S.R., Ricci, A., Paissoni, M.A., Curioni, A., Marangon, M., Mattivi, F., Arapitsas, P., Moio, L., Piombino, P., Ugliano, M., Slaghenaufi, D., Gerbi, V., Luca Rolle, L., & Versari A. (2021). Diversity of Italian red wines: a study by enological parameters, color, and phenolic indices. *Food Research International, p.110277*. https://doi. org/10.1016/j.foodres.2021.110277.

Gonda, I., Bar, E., Portnoy, V., Lev, S., Burger, J., Schaffer, A. A., Tadmor, Y., Gepstein, S., Giovannoni, J. J., Katzir, N., & others. (2010). Branched-chain and aromatic amino acid catabolism into aroma volatiles in Cucumis melo L. fruit. *Journal of Experimental Botany*, *61*(4), 1111–1123. https://doi. org/10.1093/jxb/erp390

Hayat, S., Hayat, Q., Alyemeni, M. N., Wani, A. S., Pichtel, J., & Ahmad, A. (2012). Role of proline under changing environments: a review. *Plant Signaling & Behavior*, *7*(11), 1456–1466. https://doi. org/10.4161/psb.21949

Hochberg, U., Degu, A., Toubiana, D., Gendler, T., Nikoloski, Z., Rachmilevitch, S., & Fait, A. (2013). Metabolite profiling and network analysis reveal coordinated changes in grapevine water stress response. *BMC Plant Biol*, *13*. https://doi. org/10.1186/1471-2229-13-184

Höll, J., Vannozzi, A., Czemmel, S., D'Onofrio, C., Walker, A. R., Rausch, T., Lucchin, M., Boss, P. K., Dry, I. B., & Bogs, J. (2013). The R2R3-MYB transcription factors MYB14 and MYB15 regulate stilbene biosynthesis in *Vitis vinifera*. *The Plant Cell*, *25*(10), 4135–4149. https://doi. org/10.1105/tpc.113.117127

Hong, Z., Lakkineni, K., Zhang, Z., & Verma, D. P. S. (2000). Removal of feedback inhibition of Δ^1-pyrroline-5-carboxylate synthetase results in increased proline accumulation and protection of plants from osmotic stress. *Plant Physiology*, *122*(4), 1129–1136. https://doi. org/10.1104/pp.122.4.1129

Hsiao, T. C. (1973). Plant responses to water stress. *Annual Review of Plant Physiology*, *24*(1), 519–570. https://doi. org/10.1146/annurev

Hufnagel, J. C., & Hofmann, T. (2008a). Orosensory-directed identification of astringent mouthfeel and bitter-tasting compounds in red wine. *Journal of Agricultural and Food Chemistry*, *56*(4), 1376–1386. https://doi. org/10.1021/jf073031n

Ju, Y., Yue, X., Zhao, X., Zhao, H., & Fang, Y. (2018). Physiological, micro-morphological and metabolomic analysis of grapevine (*Vitis vinifera* L.) leaf of plants under water stress. *Plant Physiology and Biochemistry*, *130*, 501–510. https://doi. org/10.1016/j.plaphy.2018.07.036

Kays, S. J. (1991). Metabolic processes in harvested products. In *Postharvest physiology of perishable plant products* (pp. 75–142). Springer.

Kopka, J., Fernie, A., Weckwerth, W., Gibon, Y., & Stitt, M. (2004). Metabolite profiling in plant biology: platforms and destinations. *Genome Biology*, *5*(6), 109. https://doi. org/10.1186/gb-2004-5-6-109

Lisec, J., Schauer, N., Kopka, J., Willmitzer, L., & Fernie, A. R. (2006). Gas chromatography mass spectrometry--based metabolite profiling in plants. *Nat Protoc*, *1(1):387-96*. https://doi. org/10.1038/nprot.2006.59

Liu, Y., Gunawan, F., Yunus, I. S., & Nakamura, Y. (2018). Arabidopsis serine decarboxylase 1 (SDC1) in phospholipid and amino acid metabolism. *Frontiers in Plant Science*, *9*, 972. https://doi. org/10.3389/fpls.2018.00972

Mandelstam, J. (1963). Protein turnover and its function in the economy of the cell. *Annals of the New York Academy of Sciences*, *102*(3), 621–636. https://doi. org/10.1111/j.1749-6632.1963.tb13664.x

Mencarelli, F, Massantini, R., Lanzarotta, L., & Botondi, R. (1994). Accurate detection of firmness and colour changes in the packing of table grapes with paper dividers. *Journal of Horticultural Science*, *69*(2), 299–304. https://doi. org/10.1080/14620316.1994.11516458

Mencarelli, F.,, Bellincontro, A., Nicoletti, I., Cirilli, M., Muleo, R., & Corradini, D. (2010). Chemical and biochemical change of healthy phenolic fractions in winegrape by means of postharvest dehydration. *Journal of Agricultural and Food Chemistry*, *58*(13), 7557–7564. https://doi. org/10.1021/jf100331z

MIPAAF (2019). *Ministero delle Politiche Agricole Alimentari e Forestali, Disciplinare di Produzione della Denominazione di Origine Controllata e Garantita dei vini "Amarone della Valpolicella", Modificato con DM 02.08.2019*. G.U. n.190 del 14.08.2019. http://www.veronissima.com/sito_italiano/amarone_della_valpolicella

Panceri, C. P., Gomes, T. M., De Gois, J. S., Borges, D. L. G., & Bordignon-Luiz, M. T. (2013). Effect of dehydration process on mineral content, phenolic compounds and antioxidant activity of Cabernet Sauvignon and Merlot grapes. *Food Research International*, *54*(2), 1343–1350. https://doi. org/10.1016/j.foodres.2013.10.016

Paronetto, L, & Mattivi, F. (1999). *Il resveratrolo in enologia e applicazione dei raggi UVC per aumentarne il tenore*.

Paronetto, L., & Dellaglio, F. (2011). Amarone: a modern wine coming from an ancient production technology. In *Advances in food and nutrition research* (Vol. 63, pp. 285–306). Elsevier. https://doi. org/10.1016/b978-0-12-384927-4.00009-9

Piombino, P., Pittari, E., Gambuti, A., Curioni, A., Giacosa, S., Mattivi, F., Parpinello, G. P., Rolle, L., Ugliano, M., & Moio, L. (2020). Preliminary sensory characterisation of the diverse astringency of single cultivar Italian red wines and correlation of sub-qualities with chemical composition. *Australian Journal of Grape and Wine Research*, *26*(3), 233–246. https://doi. org/10.1111/ajgw.12431

Possingham, J. V, Chambers, T. C., Radler, F., & Grncarevic, M. (1967). Cuticular transpiration and wax structure and composition of leaves and fruit of *Vitis vinifera*. *Australian Journal of Biological Sciences*, *20*(6), 1149–1154. https://doi. org/10.1071/BI9671149

Rauf, A., & Farshori, N. N. (2011). Microwave-induced synthesis of aromatic heterocycles. *Springer Science & Business Media*.

Reščič, J., Mikulič-Petkovšek, M., & Rusjan, D. (2016). The impact of partial dehydration on grape and wine chemical composition of white grapevine (*Vitis vinifera* L.) varieties. *Eur. J. Hortic. Sci*, *81*, 310–320. https://doi. org/10.17660/eJHS.2016/81.6.4

Revelle, W. (2020). *Psych: Procedures for psychological, psychometric, and personality research.; 2020*. https://doi. org/10.5334/jopd.25

R Core Team (2020). R: A Language and Environment for Statistical Computing; R Foundation for Statistical Computing: Vienna, Austria, 2020; Available online: https://www.r-project.org/

Rolle, L., Torchio, F., Giacosa, S., & Gerbi, V. (2009). Modifications of mechanical characteristics and phenolic composition in berry skins and seeds of Mondeuse winegrapes throughout the on-vine drying process. *Journal of the Science of Food and Agriculture*, *89*(11), 1973–1980. https://doi. org/10.1002/jsfa.3686

Roy, S., Conway, W. S., Watada, A. E., Sams, C. E., Erbe, E. F., & Wergin, W. P. (1999). Changes in the ultrastructure of the epicuticular wax and postharvest calcium uptake in apples. *HortScience*, *34*(1), 121–124. https://doi. org/10.21273/HORTSCI.34.1.121

Sanz, C., Olias, J. M., & Perez, A. G. (1996). Aroma biochemistry of fruits and vegetables. *Proceedings-Phytochemical Society of Europe*, *41*, 125–156.

Savoi, S., Wong, D. C. J., Degu, A., Herrera, J. C., Bucchetti, B., Peterlunger, E., Fait, A., Mattivi, F., & Castellarin, S. D. (2017). Multi-omics and integrated network analyses reveal new insights into the systems relationships between metabolites, structural genes, and transcriptional regulators in developing grape berries (*Vitis vinifera* L.) exposed to water deficit. *Frontiers in Plant Science*, *8*, 1124. https://doi. org/10.3389/fpls.2017.01124

Schirra, M., D'hallewin, G., Ben-Yehoshua, S., & Fallik, E. (2000). Host--pathogen interactions modulated by heat treatment. *Postharvest Biology and Technology*, *21*(1), 71–85. https://doi. org/10.1016/S0925-5214(00)00166-6

Shannon, P., Markiel, A., Ozier, O., Baliga, N. S., Wang, J. T., Ramage, D., Amin, N., Schwikowski, B., & Ideker, T. (2003). Cytoscape: a software environment for integrated models of biomolecular interaction networks. *Genome Research*, *13*(11), 2498–2504. https://doi. org/10.1101/gr.1239303

Shojaie, B., Mostajeran, A., & Ghanadian, M. (2016). Flavonoid dynamic responses to different drought conditions: amount, type, and localization of flavonols in roots and shoots of Arabidopsis thaliana L. *Turkish Journal of Biology*, *40*(3), 612–622. https://doi. org/10.3906/biy-1505-2

Slaghenaufi, D., Boscaini, A., Prandi, A., Dal Cin, A., Zandonà, V., Luzzini, G., & Ugliano, M. (2020). Influence of Different Modalities of Grape Withering on Volatile Compounds of Young and Aged Corvina Wines. *Molecules*, *25*(9), 2141. https://doi. org/10.3390/molecules25092141

Sweetman, C., Sadras, V. O., Hancock, R. D., Soole, K. L., & Ford, C. M. (2014). Metabolic effects of elevated temperature on organic acid degradation in ripening *Vitis vinifera* fruit. *Journal of Experimental Botany*, *65*(20), 5975–5988. https://doi. org/10.1093/jxb/eru343

Team, R. C. (2013). *R: A language and environment for statistical computing*. Vienna, Austria.

Theodoridis, G., Gika, H., Franceschi, P., Caputi, L., Arapitsas, P., Scholz, M., Masuero, D., Wehrens, R., Vrhovsek, U., & Mattivi, F. (2012). LC-MS based global metabolite profiling of grapes: solvent extraction protocol optimisation. *Metabolomics*, *8*(2), 175–185. https://doi. org/10.1007/s11306-011-0298-z

Tholkappian, P., Prakash, M., & Sundaram, M. D. (2001). Effect of AM-fungi on proline, nitrogen and pod number of soybean under moisture stress. *Indian Journal of Plant Physiology*, *6*(1), 98–99.

Toubiana, D., Semel, Y., Tohge, T., Beleggia, R., Cattivelli, L., Rosental, L., Nikoloski, Z., Zamir, D., Fernie, A. R., & Fait, A. (2012). Metabolic profiling of a mapping population exposes new insights in the regulation of seed metabolism and seed, fruit, and plant relations. *PLoS Genet*, *8*. https://doi. org/10.1371/journal.pgen.1002612

Vance, J. E. (2015). Phospholipid synthesis and transport in mammalian cells. *Traffic*, *16*(1), 1–18. https://doi. org/10.1111/tra.12230

Vannozzi, A., Dry, I. B., Fasoli, M., Zenoni, S., & Lucchin, M. (2012). Genome-wide analysis of the grapevine stilbene synthase multigenic family: genomic organization and expression profiles upon biotic and abiotic stresses. *BMC Plant Biology*, *12*(1), 130. https://doi. org/10.1186/1471-2229-12-130

Vannozzi, A., Wong, D. C. J., Höll, J., Hmmam, I., Matus, J. T., Bogs, J., Ziegler, T., Dry, I., Barcaccia, G., & Lucchin, M. (2018). Combinatorial regulation of stilbene synthase genes by WRKY and MYB transcription factors in grapevine (*Vitis vinifera* L.). *Plant and Cell Physiology*, *59*(5), 1043–1059. https://doi. org/10.1093/pcp/pcy045

Versari, A., Parpinello, G. P., Tornielli, G. B., Ferrarini, R., & Giulivo, C. (2001). Stilbene compounds and stilbene synthase expression during ripening, wilting, and UV treatment in grape cv. Corvina. *J Agric Food Chem*, *49*. https://doi. org/10.1021/jf010672o

Vilela, A. (2019). Use of nonconventional yeasts for modulating wine acidity. *Fermentation*, *5*(1), 27. https://doi. org/10.3390/fermentation5010027

Vrhovsek, U., Masuero, D., Gasperotti, M., Franceschi, P., Caputi, L., Viola, R., & Mattivi, F. (2012). A versatile targeted metabolomics method for the rapid quantification of multiple classes of phenolics in fruits and beverages. *Journal of Agricultural and Food Chemistry*, *60*(36), 8831–8840. https://doi. org/10.1021/jf2051569

Willetts, N. S. (1967). Intracellular protein breakdown in growing cells of Escherichia coli. *Biochemical Journal*, *103*(2), 462–466. https://doi. org/10.1042/bj1030462

Yao, L., Liu, X., Jiang, Y., Caffin, N., D'Arcy, B., Singanusong, R., Datta, N., & Xu, Y. (2006). Compositional analysis of teas from Australian supermarkets. *Food Chemistry*, *94*(1), 115–122. https://doi. org/10.1016/j.foodchem.2004.11.009

Zamboni, A., Minoia, L., Ferrarini, A., Tornielli,G. B., Zago, E., Delledonne, M., & Pezzotti, M. (2008). Molecular analysis of post-harvest withering in grape by AFLP transcriptional profiling. *Journal of Experimental Botany*, *59*(15), 4145–4159. https://doi. org/10.1093/jxb/ern256

Zenoni, S., Fasoli, M., Guzzo, F., Dal Santo, S., Amato, A., Anesi, A., Commisso, M., Herderich, M., Ceoldo, S., Avesani, L., & others. (2016). Disclosing the molecular basis of the postharvest life of berry in different grapevine genotypes. *Plant Physiology*, *172*(3), 1821–1843. https://doi. org/10.1104/pp.16.00865